

# Design of Scalloped-Bottom Thickener Tanks

John R. Buzek and Howard I. Epstein

## Introduction

Thickeners are simply large tanks, usually circular in shape, which are designed to allow settling of solids and to operate with continuous overflow of clear water and underflow of thick pulp. The dimensions of the thickener are usually such that dewatering of very fine pulps may be accomplished while still overflowing clear water.<sup>1</sup> Some thickeners such as the Genter, Hardinge and Hydrotator types combine thickening with filtering<sup>2</sup> while others such as the Dorr type are pure thickeners.<sup>1,2,3</sup>

A schematic diagram of the traction type Dorr thickener is shown in Fig. 1. This type is appropriate for tanks over 15 m (50 ft) in diameter. This tank employs a rotating raking mechanism which moves the settled material toward the central discharge. For this and other thickeners, it is common to have a shallow conical tank bottom in order to conform to the geometry of the raking mechanism, and it is often desirable to elevate the tank for ease of access to the product. When the tank does not rest on the ground, the forces resisted by the cone are large, and thick plates must be employed. The fabrication of these tanks requires temporary supports in order to erect the cone. A flat-bottomed tank could also be used because the settled material would soon form a hardened conical surface. However, because of the presence of large bending forces, even larger plate thicknesses are required than for the conical bottom.

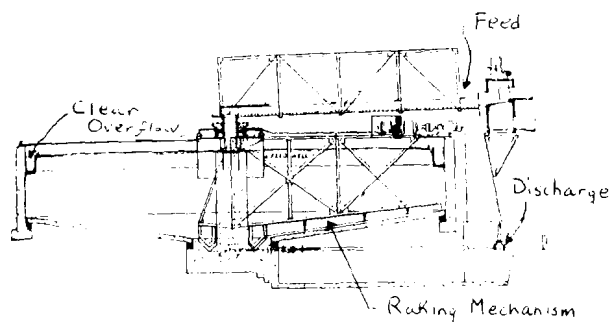


Fig. 1—Traction type Dorr thickener.

Significant cost savings often can be realized by the use of a scalloped-bottomed tank such as the one partially shown in Fig. 2. The particular scalloped bottom discussed in this paper employs radial beams forming the outline of the cone-shaped bottom. These beams are supported directly by columns. Cone segments are hung between adjacent beams. The exact geometry of these segments depends upon the cone angle and radius, the number of radial beams, and their inclination. The geometry is chosen to satisfy certain clearance restraints and to utilize the material as efficiently as possible. The resulting thickness of these segments is significantly less than that of the equivalent plate for the tank with a conical bottom. This result, along with the simpler fabrication procedures required, accounts for the cost savings associated with this design. The raking mechanism employed may be the same as for the conventional

conical bottom since the settled material soon forms a conical surface.

Determination of the internal force mechanism for the scalloped bottom leads to designs that utilized material efficiently and thus maximize the cost savings. The complicated geometry of these bottoms along with the difficulty in analyzing the structure are factors which may have limited the use of scalloped-bottomed tanks to date. When such tanks have been built, the uncertainties associated with the internal forces have led to designs that are somewhat inefficient. In this paper, equations relating the geometric parameters are presented along with simplified closed-form solutions for the internal forces in the cone segments, from which the loads applied to the beams and the loads carried to the cylindrical tank shell can be deduced. An example is presented to show the magnitude of the savings which may be realized with this configuration.

## Scallop Geometry

In order to predict the stresses and forces that occur in the scalloped-bottomed tank, it is important to have a thorough understanding of the geometry of the structure. Figure 3 shows some of the important geometric parameters for this configuration. The radius of the cylindrical tank is equal to  $R$ . The number of radial beams,  $N$ , is usually determined by the number of supports deemed necessary and the spacing requirements for ease of access to the bottom of the tank and ease of connection at their common central ring. Typically,  $N$  might equal 8 for smaller diameter tanks and become 12 or 16 with increasing diameter. The angle  $\delta$ , which lies in the horizontal plane, is given by

$$\delta = \pi/N \quad (1)$$

The radial beams are inclined by an angle  $\beta$  with the horizontal. The length of each beam,  $L$ , is then given by

$$L = R/\cos \beta \quad (2)$$

A typical cone segment  $O-A-B$  is shown in Fig. 3. Point  $O$  is the theoretical intersection of the radial beams; points  $A$  and  $B$  are at the intersection of the radial beams with the cylindrical shell; point  $M$  lies halfway between  $A$  and  $B$  on the straight line joining the two; point  $C$  is the lowest point on the intersection curve of the conical segment and the circular cylindrical shell. The length of line  $A-B$  equals  $S$  and is given by

$$S = 2R \sin \delta \quad (3)$$

**J. R. Buzek** is Chief Engineer, Brown-Minneapolis Tank, St. Paul, Minnesota 55165. **Howard I. Epstein** is Associate Professor, Department of Civil Engineering, Univ. of Connecticut, Storrs, Connecticut 06268. *SME preprint 77B48, AIME Annual Meeting, Atlanta Ga., March 1977. Manuscript Dec. 6, 1976. Discussion of this paper must be submitted, in duplicate, prior to July 31, 1979.*

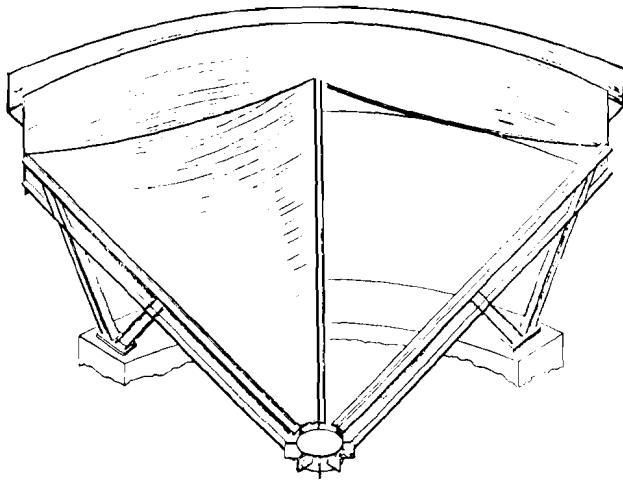


Fig. 2—Scalloped bottom layout.

The vertical separation between point C and point A, B or M is equal to  $v$ . This distance is important since it is a measure of the clearance at the edge of the tank. The value of  $v$  depends not only on the number of radial beams and their inclination, but on the geometry of the particular conical segments placed between the beams.

The slope of the plane O-A-B with the horizontal is equal to the angle  $\lambda$ . Since line O-M has a length equal to  $(L^2 - (S/2)^2)^{1/2}$  and the elevation of point A, B or M above point O is equal to  $R \tan \beta$ , using Equations (2) and (3) yields

$$\sin \lambda = \sin \beta / (1 - \sin^2 \delta \cos^2 \beta)^{1/2} \quad (4)$$

The geometry of the conical segment is shown in Fig. 4. This segment is a part of a cone having cone angle  $\alpha$ , base radius  $R_C$  and height  $h_C$ . Since the base of the cone must pass through points A and B, the cone radius and height are not arbitrary, but depend upon the cone angle through the equations

$$R_C = L \sin \alpha; h_C = L \cos \alpha \quad (5)$$

The cone segment between adjacent beams is a truncated portion of a wedge of the cone depicted. The wedge portion projects an angle  $2\phi$  on the circular cone base as shown in the section view in Fig. 4. The angle  $\phi$  can be found in terms of previously defined quantities using Equations (2), (3) and (5) since

$$\sin \phi = S/2R_C = \sin \delta \cos \beta / \sin \alpha \quad (6)$$

The wedge is truncated at the intersection of the vertical cylindrical tank wall. The plane O-A-B makes an angle  $\Theta$  with the axis of the cone where

$$\tan \Theta = R_C \cos \phi / h_C = \tan \alpha \cos \phi \quad (7)$$

The distance  $v$  may now be found by subtracting the elevation of point C from the elevation of line A-B. It follows that

$$v = R (\tan \beta - \tan \Delta) \quad (8)$$

where  $\Delta = \lambda + \Theta - \alpha$ .

In a typical problem,  $R$ ,  $N$  and  $\beta$  are specified. All that is then needed to completely define the scallop geometry is the cone angle  $\alpha$  or the cone radius or height since Equations (1)-(8) may be solved, in order, for the remaining geometric parameters.

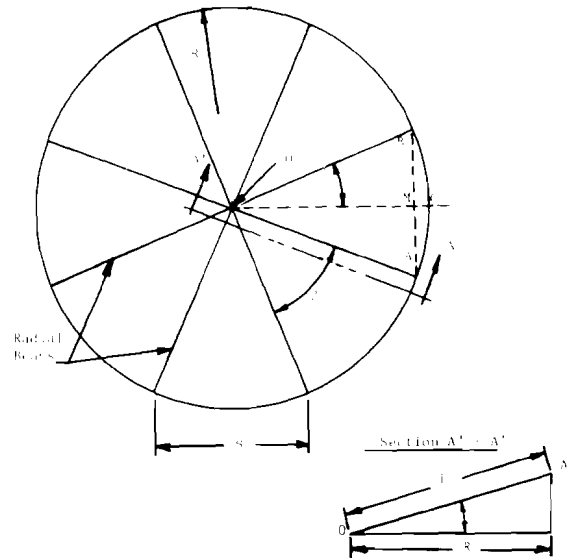
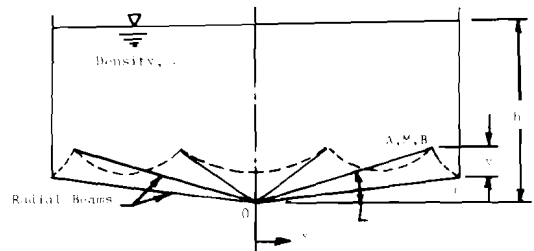


Fig. 3—Parameters of the scalloped-bottomed tank.



Typical interaction curves for the basic geometric parameters are shown in Fig. 5 wherein the following parameters are introduced:

$$V = v/R; D = R_C/R \quad (9)$$

When  $R_C$  is less than  $S/2$ , the cone cannot span adjacent radial beams and the scallop geometry is impossible. This limiting situation is equivalent to specifying a minimum value for  $D$ , as seen in Fig. 5 where

$$D_{\min} = \sin \delta \quad (10)$$

When  $D = 1$ , the cone axis is vertical,  $v = 0$  and the bottom of the tank is conical. When the line O-C is horizontal,  $V = \tan \beta$ . Since it is usually undesirable to have line O-C slope downward from point O, the line  $V = \tan \beta$  is shown as limiting the range of permissible geometries.

The use of curves similar to those given in Fig. 5 enables the designer, through a short trial and error procedure, to determine the scallop geometry which satisfies the various constraints placed on a particular problem.

### Internal Scallop Forces

The pressure acting along line O-C is given by

$$p = \rho (h - x \tan \Delta) \quad (11)$$

where, as seen in Fig. 3,  $\rho$  is the density of the contained product,  $x$  is the horizontal distance to a point along line O-C and  $h$  is the pressure head at point O.

A general expression for the pressure along any generating line of the conical segment (generatrix) involves a measure of the distance along that line as well as the inclination of the line from the horizontal. In order to simplify the analytic expression for the forces in the scallop, it is conservatively, and quite accurately, assumed that the pressure at any point on the intersection of the cone and the plane  $x = \text{constant}$  is given by Equation (11).

For the purpose of finding the internal forces in the cone segment, it is more convenient to express this pressure in terms of the distance along the cone axis,  $z$  (as shown in Fig. 4). Since

$$x \cos \lambda = z \cos \theta \quad (12)$$

the pressure can be rewritten as

$$p = q(h - Kz) \quad (13)$$

where

$$K = \tan \Delta (\cos \lambda / \cos \theta) \quad (14)$$

The forces in the conical scallop segment can be found easily since the current problem is analogous to the conical-bottomed tank shown in Fig. 6(a) for which the pressure distribution is given by

$$p = q'(h' - z) \quad (15)$$

Therefore, if

$$p' = Kq \quad (16)$$

and

$$h' = h/K \quad (17)$$

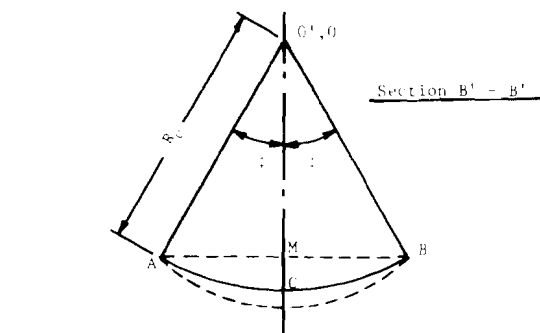
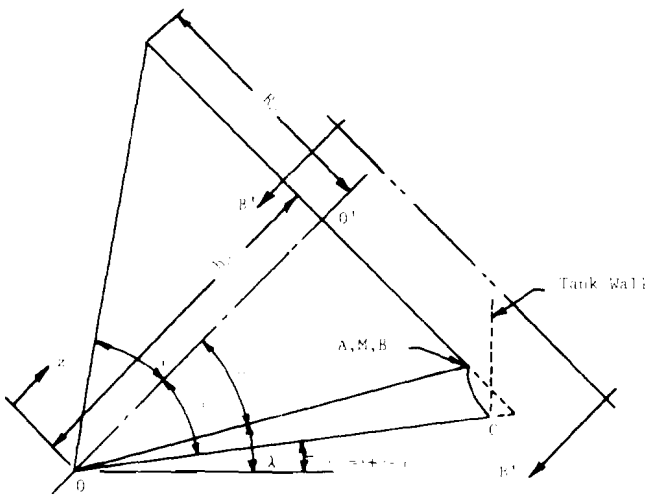


Fig. 4—Scallop cone geometry.

the forces in the conical bottom ( $z \leq h_c$ ) are equal to the corresponding forces in the conical scallop segment. The solution for the forces in the cone shown in Fig. 6(a) is well known and may be found in many standard references on shell structures.<sup>4,5</sup>

At any elevation  $z$ , the force in the direction of a cone generator (called longitudinal or meridian force) per unit length along the circumference of the circle (of radius  $z \tan \alpha$ ) is denoted by  $N_\phi$ , as shown in Fig. 6(b), and is given by

$$N_\phi = qz(h - (2/3)Kz) \tan \alpha / (2 \cos \alpha) \quad (18)$$

This relationship is easily verified by noting that the weight of the product is counteracted by the  $z$ -component of  $N_\phi$  over the circumference of the circle. The hoop force (also called ring or latitudinal force) per unit length along a generator is denoted by  $N_\theta$  and is given by the pressure times the radius of curvature in the hoop direction which yields

$$N_\theta = qz(h - Kz) (\tan \alpha / \cos \alpha) \quad (19)$$

The longitudinal force  $N_\phi$  has a maximum value at  $z = 3h'/4$ , while the maximum value of the hoop force  $N_\theta$  occurs at  $z = h'/2$ . Both of these values for  $z$  are much larger than  $h_c$  for most problems. This means that both  $N_\phi$  and  $N_\theta$  increase from zero at the center to maximum values at the intersection of the conical segment with the cylindrical tank wall. The stresses anywhere in the conical segment are obtained simply by dividing the forces  $N_\phi$  and  $N_\theta$  by the thickness of the cone at that point.

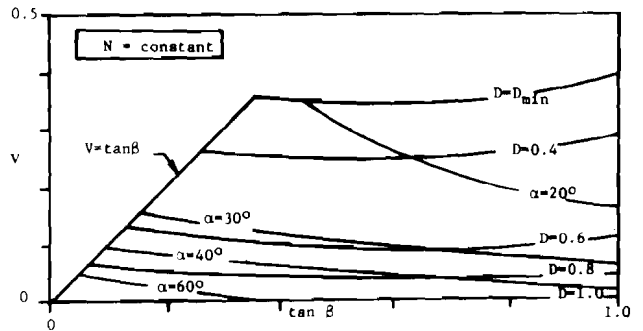


Fig. 5—Plot of scallop geometry parameters

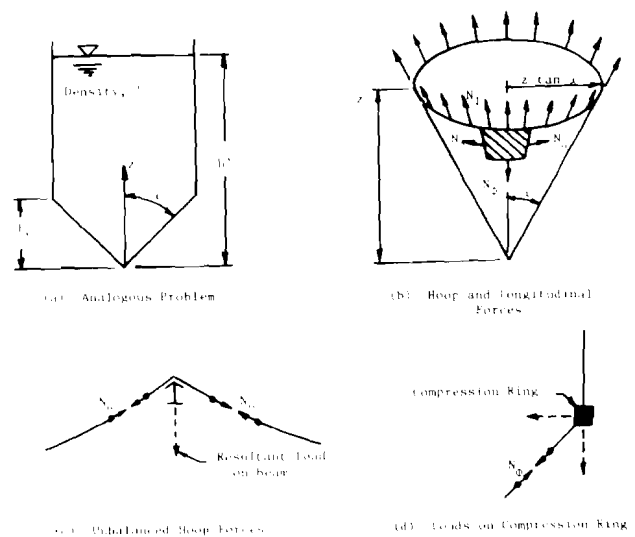


Fig. 6—Internal scallop forces.

The forces in the conical segment are transmitted to the radial beams and to the tank wall. The hoop forces have an unbalanced component at the intersection of the conical segments with the radial beams as shown in Fig. 6(c). The beams carry this force which is equal to  $2N\phi \sin \phi$  per unit length along the beam and is perpendicular to the axis of the cone.

At any section  $z = \text{constant}$  along the conical segment, the longitudinal forces  $N\phi$  may be integrated over the circular segment to give net forces perpendicular to and parallel to the cone axis. At the tank wall, these forces may be found approximately by assuming that the plane  $z = h_c$  represents the intersection of the cone with the tank wall. This is a conservative estimation of the forces since along the curved line of intersection  $z \leq h_c$  and since  $N\phi$  is a monotonically increasing function. The force resultants may be resolved into horizontal and vertical components as shown in Fig. 6(d). The horizontal component is usually resisted by a compression ring. The vertical component is transmitted through bending in the ring into the columns supporting the tank. Alternatively, the imbalance of the net internal forces from one section to the next along the cone may be considered to be all or partially resisted along the length of the radial beams. This resistance is due to the shearing forces transmitted from the edges of the conical segment to the radial beams. If these forces are properly taken into account, the compression ring may be significantly reduced in size or eliminated completely and the shear in the supporting columns may be reduced.

#### Cost Savings

A 14.0 m (46 ft) diameter tank with 2.4 m (8 ft) high walls containing a slurry having design specific gravity of 2.25 is used to compare the costs of a cone versus a scalloped-bottomed tank. This particular example was selected because Brown-Minneapolis Tank recently designed and erected five of these tanks with scalloped bottoms. The tanks were designed with eight radial beams inclined at approximately  $14^\circ$ .

The force analysis described in the previous section leads to required scallop plate thicknesses that increase from the center to a maximum of 4.76 mm ( $3/16$  in.) at the edges. For fabrication and stability purposes, the minimum size of 6.35 mm ( $1/4$  in.) is

used throughout. The cylindrical tank wall is also 6.35 mm ( $1/4$  in.) thick except for the bottom 0.69 m (27 in.) section which is increased to 19.1 mm ( $3/4$  in.) to partially act as a compression ring.

For comparison purposes, the same tank geometry is redesigned with a flat conical bottom. The design calls for a cone bottom with plate thicknesses varying from 6.35 mm ( $1/4$  in.) from the center to one-third the cylinder radius to 10.3 mm ( $13/32$  in.) over the middle third to 12.7 mm ( $1/2$  in.) for the outer third. Because of the different areas involved, this conical bottom is equivalent in weight to a plate of uniform thickness equal to 11.2 mm (0.441 in.). The cylindrical tank wall is 6.35 mm ( $1/4$  in.) except for a 1.17 m (46 in.) section 34.9 mm ( $1-3/8$  in.) thick which forms the bottom of the cylinder and a supporting skirt. Additionally, 0.711 m (28 in.) of 34.9 mm ( $1-3/8$  in.) thick plate are required to properly complete the compression ring. The flat, cone-bottomed tank contains approximately 15,900 more kg (35,000 lb) of steel than the scalloped-bottomed tank. Based upon a 1976 price of approximately \$1.21/kg (\$0.55 per lb) of in-place steel, the cost differential amounts to 19 thousand dollars.

Tanks of larger diameter would show even greater savings. There are no tank diameter limitations for the use of a scalloped bottom except that for a fixed number of radial beams, the stability of the individual scallop sections would eventually be a problem. However, this difficulty could be eliminated by increasing the number of radial beams.

#### References

- <sup>1</sup>Richards, R. H. and Locke, C. E., *Textbook of Ore Dressing*, 3rd ed., McGraw-Hill, New York, 1940, pp. 160-163.
- <sup>2</sup>Gaudin, A. M., *Flotation*, 1st ed., McGraw-Hill, New York, 1932, pp. 407-410.
- <sup>3</sup>Peele, R., *Mining Engineers' Handbook*, 2nd ed., Wiley, London, 1927, pp. 1941-1942.
- <sup>4</sup>Timoshenko, S. and Woinowsky-Kreiger, S., *Theory of Plates and Shells*, 2nd ed., McGraw-Hill, New York, 1959, pp. 439-440.
- <sup>5</sup>Harvey, J. F., *Theory and Design of Modern Pressure Vessels*, 2nd ed., D. Van Nostrand, Toronto, 1971, pp. 41-42.

## Geologic Aspects of Recent Exploration and Development in the Park City Silver-Lead-Zinc District, Utah

A. J. Erickson, Jr. and W. J. Garmoe

**Abstract**— In mid-1970, Park City Ventures, a Utah partnership of Asarco and the Anaconda Company, initiated a six-phase exploration and development program in the Park City District, Utah. Geologic studies had delineated a number of exploration targets in several areas of the district. Discovery of ore in any of the target areas and continued favorable downdip development below then productive ore bodies would allow for reserve expansion and mill construction. The targets were: replacement mineralization in the Mississippian Humbug formation below productive ore bodies on the east flank of the Park City anticline; replacement mineralization in the Humbug formation in an unexplored fault block in the footwall of the Hawkeye structure on the east flank of the anticline; vein and replacement mineralization along the Silver Fissure; potentially

higher grade replacement mineralization in the Humbug formation in a theorized structural block on the west flank of the anticline beneath the Ontario vein; replacement mineralization in the Permian Park City formation in the West End shaft area of the Silver King mine; vein mineralization along the Back vein in the Judge mine. In 1971 the Judge and Silver King Projects were suspended, due to a 30% cutback in the exploration budget. In spite of the cutback additional reserves were developed below the Humbug East Flank ore bodies; a major zone of ore grade mineralization was discovered along the Silver Fissure; five new ore bodies were found in the Humbug and Doughnut formations on the west flank of the anticline beneath the Ontario vein. First concentrates were shipped from a new mill in May 1975.